Evolution, 2025, **XX(XX)**, 1–15
https://doi.org/10.1093/evolut/qpaf020
Advance access publication 3 February 2025
Original Article

Feather evolution following flight loss in crown group birds: relaxed selection and developmental constraints

Evan T. Saitta[1], Lilja Balaji[2], Jonathan S. Mitchell[3], Peter J. Makovicky[1,4]

[1]Life Sciences Section, Field Museum of Natural History, Negaunee Integrative Research Center, Chicago, IL, United States
[2]Department of Geosciences, University of Cincinnati, Cincinnati, OH, United States
[3]Department of Biology, Coe College, Cedar Rapids, IA, United States
[4]Department of Earth & Environmental Sciences, University of Minnesota, Minneapolis, MN, United States

Corresponding author: Field Museum of Natural History, Negaunee Integrative Research Center, Life Sciences Section, 1400 S Lake Shore Dr, Chicago, IL 60605, United States. Email: evansaitta@gmail.com

Abstract

Feathers are complex structures exhibiting structural/functional disparity across species and plumage. Flight was lost in >30 extant lineages from ~79.58 Ma–15 Ka. Effects of flight loss on senses, neuroanatomy, and skeletomusculature are known. To study how flightlessness affects feathers, we measured 11 feather metrics across the plumage of 30 flightless taxa and their phylogenetically closest volant taxa, with broader sampling of primaries across all orders of crown birds. Our sample includes 27 independent flight losses, representing nearly half of extant flightless species. Feather asymmetry measured by barb angle differences between trailing and leading vanes decreases in flightless lineages, most prominently in flight feathers and weakest in contour feathers. Greatest changes in feather anatomy occur in older flightless lineages (penguins, ratites). Comparative methods show that many microscopic feather traits are not dramatically modified after flightlessness compared to body mass increase and relative wing and tail fan reduction. Changes involved with greater vane symmetry show stronger shifts, however. Relaxing selection for flight does not rapidly modify feather flight adaptations, apart from asymmetry. Developmental constraints and relaxed selection for novel feather morphologies may explain some observed changes. Macroscopic changes to flight apparati (skeletomusculature, airfoil size) are more evident in recently flightless taxa and could more reliably detect flightlessness in fossils, with increased feather symmetry as a potential microscopic signal. We observed apical modification in later stages of feather development (asymmetric displacement of barb loci), while morphologies arising during early developmental stages are only altered after millions of years of flightlessness.

Keywords: relaxed selection, macroevolution, developmental constraints, natural selection, birds, feathers

Introduction

With 11,000–18,000 species (Barrowclough et al., 2016), a global distribution across many habitats and ecological niches (Mitchell & Makovicky, 2014), and an evolutionary history stretching over 150 million years (von Meyer, 1861), birds are among the most successful vertebrates. Although many adaptations help explain their evolutionary success, a key adaptation is feathering.

Flight is a major aspect of feather evolution but has been independently reversed in many bird lineages throughout evolution (Roots, 2006). Flight loss thus allows us to study relaxed selection, where partial or total functional loss leads to vestigialism or loss of traits (Lahti et al., 2009), on structurally and developmentally complex traits. Even considering just extant lineages, occurrences of flight loss span three orders of magnitude of time. Ostrich (*Struthio camelus*) ancestors losing flight ~79.58 Ma (Yonezawa et al., 2017), while Fuegian steamer ducks (*Tachyeres pteneres*) lost flight as recently as 15 Ka (Fulton et al., 2012). This wide range means comprehensive sampling informs upon evolutionary rates across macroevolutionary time, with early and late evolutionary stages of anatomy represented in the dataset. Some poor-flying species even appear to be in the process of losing flight (i.e., "incipiently flightless"), such as the extant New Zealand saddleback (*Philesturnus*) (Taylor et al., 2007) or the recently extinct, semiaquatic New Zealand merganser (*Mergus australis*) (Livezey, 1989).

Flight can also be lost during ontogeny—the flightless adult giant coot (*Fulica gigantea*) retains volant juveniles (Fjeldså, 1981; Livezey, 2003) (coded here as flightless). In contrast, only the heaviest males of the flying steamer duck (*Tachyeres patachonicus*) are flightless (Humphrey & Livezey, 1982; Livezey, 2003) (coded here as volant). Some taxa are seasonally flightless due to simultaneous/synchronous molting (Dial & Heers, 2021). Although some domestic species are flightless/poor flyers because of artificial selection (Feng et al., 2014; Miller, 1956), we omit these.

Flight loss often occurs in two ecological contexts. Terrestrial flight loss is often seen in "founder" events where ancestors occupy new regions, such as islands without predators (Clout & Craig, 1995; Wright et al., 2016). Alternatively, some bird lineages lost flight upon transitioning to semiaquatic ecologies (Elliott et al., 2013; Fish, 2016). These scenarios are possibly related to heavily discussed phenomena in evolutionary biology—island evolutionary dynamics (e.g., island dwarfism or gigantism [Lomolino et al., 2013]) and secondarily aquatic convergent evolution (Kelley & Pyenson, 2015).

Received December 11, 2023; revisions received December 18, 2024; accepted January 30, 2025

Associate Editor: Kjetil Voje; Handling Editor: Miriam Zelditch

The effect of flight loss on brain size (Ksepka et al., 2020), sensory capacity (Torres & Clarke, 2018), and skeletomusculature (e.g., Cubo & Arthur, 2001; Watanabe et al., 2021) of birds has been studied, but less work exists on feathers themselves, especially at microscopic levels (McGowan, 1989). We examine feather variation in extant/recently extinct birds to characterize changes in feathers upon flight loss. We study both flight and contour feathers to judge the impact of flight loss across the plumage and better detect morphological changes tightly correlated to flight loss.

Another unknown is the rate feathers evolve at after flight loss, especially compared to better-documented morphological changes (e.g., in the skeletomusculature). Under one hypothesis, feathers, which are morphologically plastic over macroevolutionary timeframes, could evolve rapidly when selection for flight and predation pressure is relaxed. Alternatively, metabolically cheap feathers might evolve slower than metabolically expensive bone and muscle of the flight apparatus if feathers are selectively neutral (Lahti et al., 2009) following flight loss and/or constrained by their complex development (Prum, 1999).

We test several hypotheses about feather evolution after flight loss:

(1) If relaxed selection from flight loss accelerates feather evolution, morphological changes in feather morphology should be more readily observed in flight feathers compared to contour feathers.

(2A) If feathers are evolutionarily plastic, they might evolve rapidly after relaxed selection from flight loss compared to the skeletomusculature. (2B) Alternatively, if feathers are metabolically cheap and/or developmentally constrained, they might persist over long timescales, evolving slower than the skeletomusculature following flight loss.

(3) The rates at which different feather traits evolve after relaxed selection from flight loss might vary, especially if feathers are developmentally constrained and/or their different traits experience novel selective pressures (e.g., interlocking barbules and closed vanes for lift, feather asymmetry for reduced drag, long filaments for thermoregulation, tight hooklet/barbicel interlocking for water repellency).

(4) If ecological context (i.e., terrestrial versus semiaquatic) imparts different selective pressures after flight loss, then evolutionary patterns or rates might differ between terrestrial and semiaquatic flightless birds. Due to disparate modes of semiaquatic locomotion in birds, we were conservative in our conclusions regarding this hypothesis.

(5) If flight loss follows typical dynamics of relaxed selection, then we can interpret feather evolution according to common models of trait value versus fitness (Lahti et al., 2009), but their structural/developmental complexity might impact such models.

Methods

Taxon sampling

There are ~64 species of extant flightless birds, ~28% of which are penguins (Sphenisciformes). Ecologically, ~59% of flightless species are terrestrial and ~41% are semiaquatic (Roots, 2006). We examined bird skins at the Field Museum of Natural History and American Museum of Natural History. Our sample (83 total taxa, 307 feathers) contained 30 taxa (nine orders) fully flightless as adults (Palaeognathae, Gruiformes, Psittaciformes, Charadriiformes, Anseriformes, Podicipediformes, Suliformes, Sphenisciformes, Passeriformes), nearly half of which are rare/threatened (IUCN, 2022). Our sample is ~57% terrestrial and ~43% semiaquatic, resembling the ecological breakdown among all living flightless species.

We reduced sampling of flightless species within nonvolant lineages to avoid redundancy (Supplementary Material, Section 1): our dataset is only 10% penguins, while broadly covering major penguin lineages (*Spheniscus*, *Eudyptes*, *Aptenodytes* [Ksepka et al., 2006]). Only one species from each of the five living genera (13 total species) of ratites (i.e., flightless Palaeognathae) is included because they represent only four independent losses of flight (Yonezawa et al., 2017): (1) *Struthio camelus*, (2) *Rhea americana*, (3) *Dromaius novaehollandiae*/*Casuarius unappendiculatus*, and (4) *Apteryx australis*.

Six of our flightless taxa are recently extinct (*Porzana sandwichensis*, *Porzana palmeri*, *Gallinula nesiotis*, *Xenicus lyalli*, *Podilymbus gigas*, *Pinguinus impennis*). One recently extinct species was poor-flying/"incipiently flightless" (*Mergus australis*).

For each flightless/"incipiently" flightless taxon, we included its phylogenetically closest volant taxon for sister taxon comparisons. For penguins, we included three volant species of tubenoses (Procellariiformes), representing major lineages within that clade (*Oceanites oceanicus*, *Pelecanoides urinatrix*, *Diomedea immutabilis*).

We expanded sampling of crown birds to include at least one species from each commonly recognized order (Reddy et al., 2017) All these broadly sampled species are volant, except for *Mesitornis unicolor*, whose flight capabilities are unknown.

Data acquisition

Macro- and microscopic measurements were made on skins of size/proportions, densities, and positions of various skeletal, scale, and feather traits (Supplementary Data S1), supplemented with values from the literature (e.g., species body mass was frequently taken from Dunning [2008]). Chosen variables (Supplementary Material, section 3) were considered relevant from prior studies (e.g., Cubo & Arthur, 2001; Feo et al., 2015), sufficient to describe anatomy, and practical to measure. Macroscopic traits included body mass, wing length from the wrist to tip of the longest primary, and tail fan length from the posterior end of pygostyle to tip of the longest rectrix. Data, scripts, and archiving are available at https://github.com/paleomitchelljs/FeatherEvo and in Supplementary Data S4.

Equipment

Macroscopic traits were measured with analog calipers, digital calipers, and measuring tape. Microscopic observations of feathers utilized a Dino-Lite Edge AM73915MZTL (10X~140X; 5.0MP; USB 3.0) Digital Microscope with calibrated scalebar (supplemented with a physical scale bar) with a maneuverable Dino-Lite MS36A-C2 adjustable precision mount and clamp. Measurements were taken from micrographs using Adobe Photoshop (version 20.0.6).

Feathers sampled

For clades containing flightless taxa, five feathers across the body were measured: longest primary remex, dorsal-most

tertial remex, dorsal-most rectrix, and dorsal and ventral contours from roughly the middle of the torso. For orders without flightless taxa, only the longest primary remex was measured, assuming that effects of flight loss are strongest in them (a hypothesis ultimately supported). For internal consistency, we define "trailing" vanes of contour feathers as those more medial and "leading" vanes as those more lateral, even though these terms are inapplicable to feathers that do not generate lift.

Each feather was manipulated by hand for maximum exposure from the plumage. Paper was placed underneath for contrast. Barbs were exposed using a metal pick and sewing pins.

Observations of each feather

Observations were made at apical, middle, and basal regions along the exposed extent of the rachis (Supplementary Data S1). We focused on the middle region because the apex is often damaged in museum specimens and exhibits high asymmetry between comparable feather positions on left and right sides of an individual. Basal regions would sometimes include plumulaceous regions, depending on how much the feather could be exposed.

Feather metrics of greatest interest are shown in Figure 1A (for kiwi, a barb pair with at least one well-developed barb was measured [Figure 1B; Supplementary Material, Section 2]). Barbules and mid-barb width were measured only on the trailing barb, since the trailing vane has a greater area than the leading vane on flight feathers, relating to the wing's lift surface. To control for overall feather size and position along the rachis' length, linear feather metrics (rachis width, mid-barb width on trailing barb, leading barb length, trailing barb length, and distal barbule length on trailing barb) were divided by the length from the apical most barb node to the measured barbs. Although some groups (e.g., penguins, ratites) may contain outliers, body mass and feather length positively correlate in flying species (Sullivan et al., 2017). In our dataset, feather size (i.e., rachis length at middle region) shows greater correlation to taxon body mass than does feather asymmetry (i.e., difference in trailing and leading barb angle at middle region), suggesting that body size does not confound our conclusions (Supplementary Material, Section 9; Supplementary Data S3). Proximal barbule length was not examined due to difficulties in manually unfurling tightly overlapping barbules in many taxa.

Error in barb orientation can result from curvature at the base of barbs or manipulation (Feo et al., 2016). Barb angle differences were used to measure feather asymmetry at a given barb pair along the rachis, controlling for distortion at that position along the rachis or for variation in measurement. Feather asymmetry equaled the angle of the trailing barb subtracted by the angle of its paired leading barb—consistent with developmental models of feather asymmetry (Feo & Prum, 2014). Lower values indicate greater symmetry. Trailing barb angles are typically greater than leading barb angles in volant birds (Feo et al., 2016), and greater asymmetry is indicated by larger positive differences in barb angles. Other studies often measure feather asymmetry using the width of the leading versus trailing vanes perpendicular to the rachis. As a fractal structure, feather asymmetry is also reflected in other metrics (e.g., barb densities or barb lengths on leading versus trailing vanes).

Filament densities were measured as the number of filaments per unit distance (i.e., number of barbs or barbules per mm along rachis or barb, respectively). This approach does not consider scaling (i.e., similarly shaped feathers can vary in density due to size alone) but is appropriate with feather

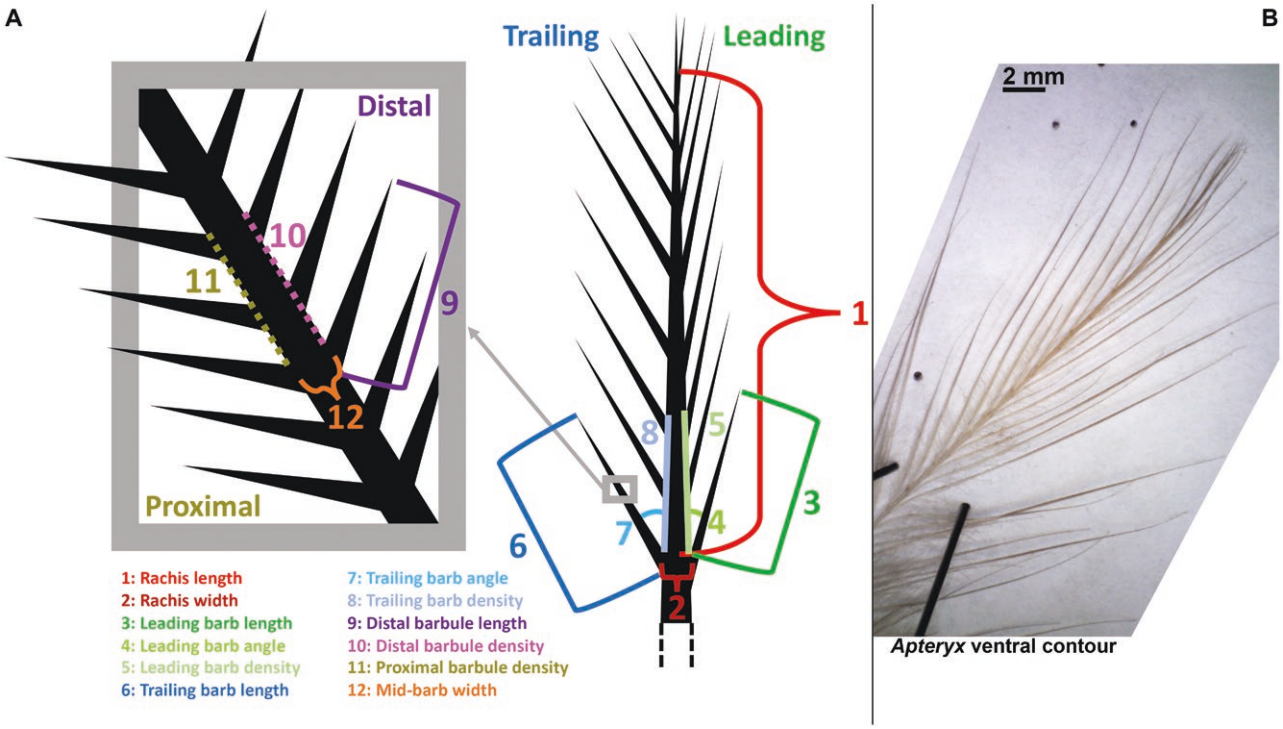

Figure 1. Measured feather morphology. (A) Key microscopic feather metrics. We focus on the midpoint of the exposed rachis on the museum skin (i.e., full extent of exposed feather [dashed lines] is roughly double value #1). (B) *Apteryx australis* ventral contour showing semialternating pattern of barb development and partial barbule loss along barb farthest from the rachis.

Table 1. Barb and distal barbule (~mid-length along trailing vane's barb) expression across middle and basal feather regions in ratites.

		Middle region		Basal region	
		Barbs	Barbules at mid-barb (trailing vane)	Barbs	Barbules at mid-barb (trailing vane)
Struthio 79.68 Ma	Primary	X	X	X	X
	Tertial	X	X	X	X
	Rectrix	X	X	X	X
	Dorsal contour	X	X	X	X
	Ventral contour	X	X	X	X
Rhea 70.62 Ma	Primary	X	O	X	X
	Tertial	X	X	X	X
	Rectrix	X	X	X	X
	Dorsal contour	X	X	X	X
	Ventral contour	X	X	X	X
Casuarius 66.69 Ma	Primary	O	O	O	O
	Tertial	X	O	X	X
	Rectrix	X	O	X	O
	Dorsal contour	X	X	X	X
	Ventral contour	X	O	X	O
Dromaius 66.69 Ma	Primary	X	O	X	X
	Tertial	X	X	X	X
	Rectrix	X	O	X	O
	Dorsal contour	X	X	X	X
	Ventral contour	X	X	X	X
*Apteryx** 62.01 Ma	Primary	X	X	X	X
	Tertial	X	X	X	X
	Rectrix	X	O	X	X
	Dorsal contour	X	X	X	X
	Ventral contour	X	X	X	X

Note. Estimated divergence ages from Yonezawa et al. (2017). X = presence. O = absence. **Apteryx* often has partial barbule loss along the barb farthest from the rachis (even when barbules are present at mid-length) and has semialternating barb developmental patterns.

development (Prum, 1999). It assumes larger feathers do not develop isometrically, but rather allometrically (consistent with models by Chernova & Kiladze, 2019; Lin et al., 2006; Maderson & Alibardi, 2000; Prum, 2005; Prum & Brush, 2002; Sawyer et al., 2003). Unscaled filament density values reflect the rate of branching during development. To account for size confounding, we also analyzed scaled densities of barbs and barbules in primaries (Supplementary Material, Section 8), where density was multiplied by rachis width at that position, converting filaments/mm into filament counts.

Analysis

We triangulated (Munafò & Smith, 2018) using simple and sophisticated statistical analyses with increasing phylogenetic control, rerun under varying conditions (Supplementary Material, Sections 4–7; Supplementary Data S2–S4). We compare relative effect sizes, rather than solely relying on arbitrary thresholds of statistical significance (Amrhein et al., 2019). Given available sample sizes, we made broad comparisons (e.g., volant versus flightless, recent versus ancient divergences, inter-order differences, terrestrial versus semiaquatic). Semiaquatic ecologies were coded 0 to 5 inspired by Fish, (2016): 0, terrestrial; 1, adaptive surface hindfeet paddling (beyond wading or ability to swim); 2, surface wing paddling (i.e., "steaming") with surface hindfeet paddling; 3, underwater hindfeet rowing; 4, asymmetrical underwater flight; 5, symmetrical underwater flight. However, fine parsing leads to small sample sizes per category, so separate analyses lumped categories 1–5 into a single semiaquatic ecological designation.

Analyses were performed using R coding language (RStudio version 1.3.1056). We started with sister taxon comparisons between volant taxa and their phylogenetically closest flightless relative by subtracting the value of the volant taxa (e.g., a density) from that of their sister flightless taxa: $\Delta = \text{Metric}_{\text{Flightless}} - \text{Metric}_{\text{Volant}}$. For penguins, volant values were averaged from three tubenoses (*Oceanites oceanicus*, *Pelecanoides urinatrix*, *Diomedea immutabilis*). Data were normalized during principal component analysis (PCA).

Data were not log-transformed when feathers without barbules/barbs would yield undefined values (i.e., PCA of linear metrics of rachis, barbs, and barbules, or shifts in density and barb angle symmetry), allowing for inclusion of taxa lacking barbs/barbules (i.e., some ratites [Table 1]), although the data was still normalized during PCA. PCA here reveals positions of taxa relative to each other within the morphospace, not absolute distances between taxa.

Phylogenetic comparative methods (PCM)

A series of phylogenetically controlled comparisons tested how rapidly traits changed after flight loss (Supplementary

Data S4). Using the phylogeny from Jetz et al. (2012) combined with the Gruiformes phylogeny from Garcia-Ramirez and Matzke (2021), we added recently extinct taxa and dates to their appropriate branches at a stochastically determined time. We repeated this procedure 100 times, creating a set of trees for 82 living (cassowary dropped because 0 values of various primary metrics cannot be log-transformed) and recently extinct taxa. We then employed stochastic mapping (Revell, 2012) to generate timings for flight loss along the tree. Transition rates were set to be unidirectional (flight could be lost but not re-evolved). The ancestral state for crown birds was fixed as volant.

Using this set of calibrated trees, we compared rates of change across a suite of macroscopic traits (supplemented from literature) and microscopic traits at the middle region of the exposed primary remex.

We compared the overall distributions of these macroscopic and microscopic traits between flightless and volant taxa without phylogenetic correction. We then compared 14 volant and flightless sister pairs in a strict sense. We looked for differences in rates between macro and microscopic traits by fitting one- and two-rate Brownian motion models using the R package OUwie (Beaulieu et al., 2012, 2016) to each of our 100 stochastically mapped phylogenies for each mean-centered, deviation-standardized trait. We accounted for measurement error for each trait by using maximum species standard deviation for each macroscopic trait from Weeks et al. (2020). We used maximum within-species standard error for each microscopic trait, estimated by measuring these traits on five flightless and five volant specimens of *Fulica* to assess the uncertainty around each trait.

Finally, we used a set of phylogenetic Bayesian regressions to evaluate changes in traits upon onset of flightlessness (Bürkner, 2017, 2018, 2021; de Villemereuil et al., 2012; Fuentes-G et al., 2020; Kruschke, 2011). These two-slope, two-rate phylogenetic mixture model regressions (MM) were fit using the R package RJAGS (Fuentes-G et al., 2020). These mixtures allowed lambda (phylogenetic signal) to vary, along with the evolutionary rates, intercepts, and slopes for flightless and volant species. We set priors following Fuentes-G et al. (2020), and all #Beta parameters had priors centered at 0, allowing us to test if the data support different regression structures (slopes & intercepts) as well as different rates for volant and flightless taxa. These rate estimates are separate from the rate estimates using OUwie described above; the MM rate estimates are on the direct trait values rather than standardized ratios and do not incorporate measurement error as our other analyses did. We performed these mixture model (MM) regressions for the relationship between wing length as a function of body mass, as well as for the leading barb angles, lengths, and densities being a function of the trailing values. We compared estimates of the intercepts, slopes, and evolutionary rates between volant and flightless lineages using the highest density intervals of the Bayesian posteriors via the R package HDInterval (Meredith & Kruschke, 2022).

Sampling error

Sampling error and inter-individual variation (often modeled phylogenetically as error) were examined to the extent possible given our dataset (Supplementary Data S5). We evaluated inter-individual variance in our estimates of phylogenetic rate across traits by using the greatest measured standard error in each feather trait from 10 specimens of *Fulica*, increasing uncertainty and support for the simpler one-rate Brownian motion model over the more complex two-rate model. Measurement error itself was examined by comparing the same measurements between observers, within and between feathers of a single individual, and between individuals of a single species.

Limited multiindividual sampling due to difficulty of measuring fine-scale feather traits from species, especially rare species, is common. Considering feather asymmetry, Feo et al. (2015) used a single specimen for each taxon, while Kiat and O'Connor (2024) measured three individuals, or less individuals for rarer taxa (e.g., flightless taxa).

Results

PCA of linear feather metrics across the entire plumage without phylogenetic control

PCA of all feathers in the sample, including those from clades that lack flightless taxa (Figure 2), shows that flightless taxa can have diverse feather morphologies compared to volant taxa in terms of their spread across the morphospace, especially along PC2 which describes rachis width (Figure 2A). Some flightless taxa have longer barbs and barbules, but two ventral contours from two volant species have the lowest PC1 values indicative of long barbs and barbules. The poor-flying *Mergus australis* does not show extreme feather morphologies (i.e., PC values near origin and close to most of the other feathers in the sample). Penguins often have relatively wider filaments (high PC2), especially in their rachis, while grebes and rails have some feathers with very long filaments (low PC1) (Figure 2B). A trend exists from relatively shorter and/or wider filaments to longer and/or thinner filaments according to feather position in the following descending order: primary, rectrix, tertial, dorsal contour, ventral contour (Figure 2C). Semiaquatic taxa potentially show wider filaments compared to terrestrial taxa, with penguins at very high PC2 values dominated by large rachis width (Figure 2D). The results are consistent when repeating PCA under varying initial conditions (i.e., with and without "long branch" clades flightless for 10's of millions of years or with and without clades lacking flightless taxa [Supplementary Material, Section 4]).

Feathers in anciently diverging flightless lineages

Penguins often have relatively wider filaments than their volant relatives, yielding small, stiff, scale-like feathers with very wide rachides (Figure 2B).

Ratites, however, show diverse shifts from their volant tinamou relative in their primaries (Supplementary Material, Section 4). Some exhibit shortened filaments or loss of filaments, as in quill-like cassowary (*Casuarius*) primaries lacking barbs and barbules. Other species evolve longer filaments, such as ostrich (*Struthio*) barbs and barbules and emu (*Dromaius*) barbs. Other filament patterns are summarized in (Table 1). The oldest diverging flightless ratites (i.e., *Struthio* and *Rhea*) are not more likely to have widespread filament loss than more recent divergences. The more recently diverging *Dromaius* shows barbule loss alongside lengthening barbs.

Feather asymmetry in sister taxon comparisons

Strong shifts in feather asymmetry related to flightlessness occur in primaries, revealing decreased asymmetry with flight loss (Figure 3C–G). The trend is most

prominent in the primaries of ratites, penguins, and potentially auk (although sample size is limited) (Figure 3A and B).

The pattern (barring limited sample sizes) is less apparent in ducks (Anseriformes), cormorants (Suliformes), and grebes (Podicipediformes), which are not underwater "flyers."

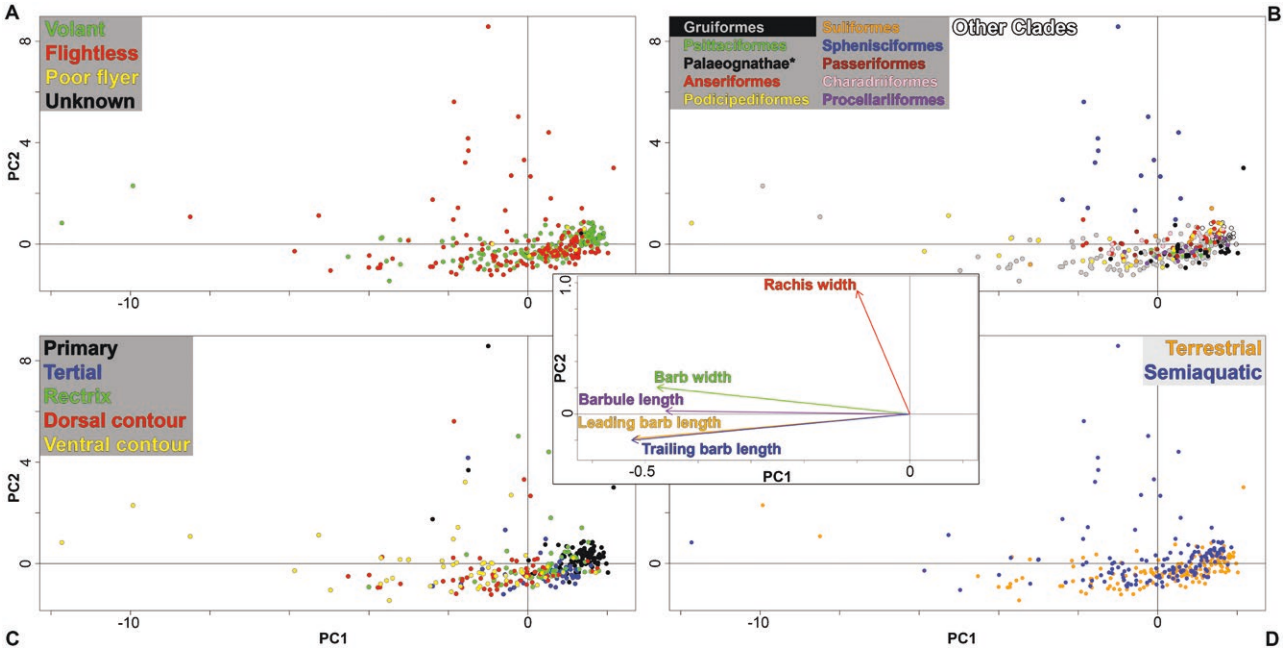

Figure 2. Principal component analysis of all feathers studied (including clades lacking flightless taxa) without phylogenetic control. PC1 and PC2 explain ~63.63% and ~21.06% of the variation, respectively. Feathers categorized by (A) flight capability, (B) clade (clades without flightless taxa in open circles; **Apteryx* are black squares to indicate their position varies depending on barb pair selected due to semialternating barb developmental pattern), (C) feather position on body, and (D) ecology. Center inset shows loading plot for the five linear metrics on PC1 and PC2. Each metric is divided by rachis length from apical most node to middle barb pair measured. $N = 307$ feathers, 83 taxa.

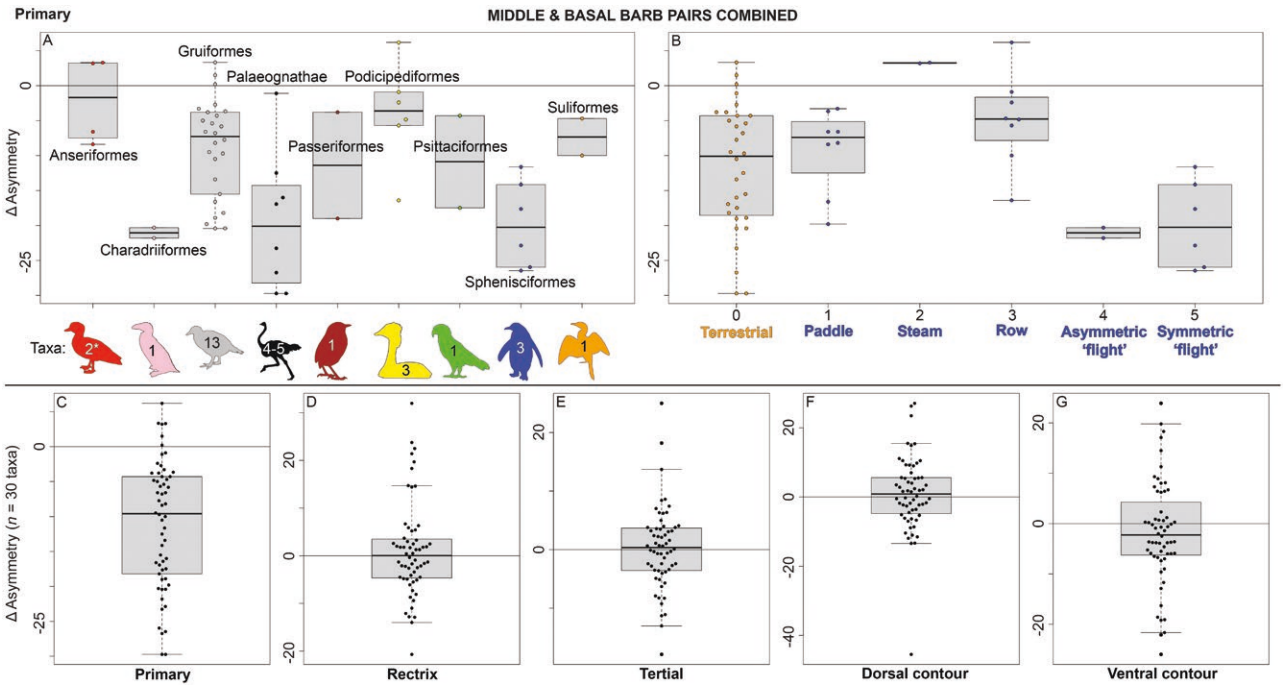

Figure 3. Shifts in feather asymmetry (i.e., trailing barb angle minus leading barb angle) of flightless taxa from their closest volant relative(s). Data combined from middle and basal barb pairs. (A) Primaries according to clade. (B) Primaries according to ecology and swim style. Total feather distributions for, (C) primaries, (D) rectrices, (E) tertials, (F) dorsal contours, and (G) ventral contours. In flightless semiaquatic taxa, "paddle" refers to surface hindlimb paddling, "steam" refers to surface "steaming" of steamer ducks, "row" refers to underwater hindlimb rowing, and "flight" refers to underwater forelimb strokes. *Poor-flying or flightless anseriform *Mergus australis* excluded. Number of taxa for Palaeognathae varies from 4 to 5 because *Casuarius* primaries lack barbs. $N = 60$ barb pairs from 30 taxa for all except the primary, which has $N = 58$ barb pairs from 29 taxa. Boxplots show median, 1st quartile, and 3rd quartile. Whiskers extend to maximum and minimum, expect for outliers outside 1.5 times the interquartile range.

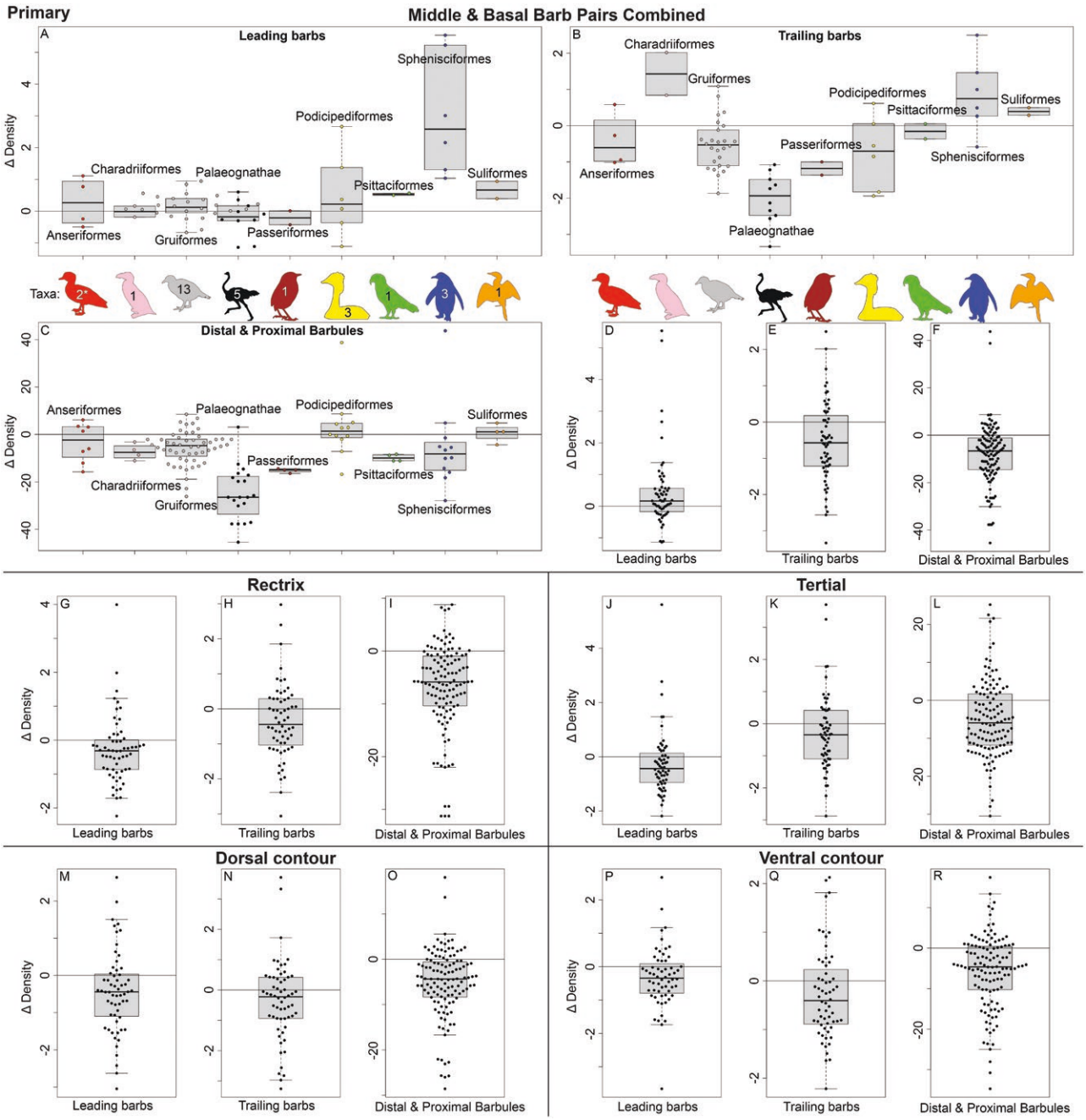

Figure 4. Shifts in raw filament densities of flightless taxa from their closest volant relative(s). Data combined from middle and basal barb pairs. (A) Primary leading barbs. (B) Primary trailing barbs. (C) Primary distal and proximal barbules on trailing barbs. Total distributions for leading barbs, trailing barbs, and distal and proximal barbules on trailing barbs for, (D)–(F), primaries, (G)–(I), rectrices, (J)–(L), tertials, (M)–(O), dorsal contours, and, (P)–(R), ventral contours. *Poor-flying or flightless anseriform *Mergus australis* excluded. $N = 60$ leading or trailing barb density measures from 30 taxa; 120 distal and proximal barbule density measures on 60 trailing barbs from 30 taxa. Boxplots show median, 1st quartile, and 3rd quartile. Whiskers extend to maximum and minimum, expect for outliers beyond 1.5 times the interquartile range.

Flightless ducks show less of a shift toward symmetric feathers than do other flightless taxa, with steamer ducks potentially showing increased asymmetry from their nearest flying relative despite being flightless. This limited observation might run counter to the notion that flight loss inevitably leads to greater feather symmetry (Feo et al., 2015; McGowan, 1989).

Filament densities in sister taxon comparisons

When comparing shifts in raw filament densities between flightless taxa and their phylogenetically closest volant taxa, densities of both barbs and barbules often decrease with flight loss (Figure 4E–R), apart from leading vane barbs on primaries (Figure 4A and D). Decreasing raw densities could be confounded by increased size in flightless taxa. In primaries, ratites show the most prominent decreases in barb and barbule densities, while penguins show the most positive shifts in barb densities (Figure 4B and C).

When barb and barbule densities are scaled to feather size (Supplementary Material, Section 8), results broadly support the unscaled observations. After scaling density values to

rachis width, barbule packing as well as leading and trailing barb packing consistently decrease after flight loss in all clades. This is true even in penguins, whose unscaled densities are very high and whose rachides are very broad compared to their overall feather size. Penguins do however show minor shifts in scaled density values, whereas ratites can show the most dramatic decreases in scaled density values, especially in barbules. Finally, scaled densities show lesser shifts in leading barb packing compared to trailing barb packing—consistent with unscaled results where a distribution centered around an increased (i.e., positive) shift in density was only seen in leading barbs of primaries.

Phylogenetic comparative methods

Rates of macroscopic versus microscopic trait evolution

We hypothesized that, upon flight loss, macroscopic traits typically shift earlier and with greater effect size (i.e., more prominently) than microscopic feather traits (Supplementary Material, Section 7). For these analyses, we incorporated intraspecific variation and used traits on the same scale (mean-centered divided by interspecific standard deviation) to directly compare estimated rates across different traits. Both one-rate and two-rate Brownian Motion models were fit to 100 different stochastically mapped trees for each trait. Averages across these 100 stochastically mapped trees are presented here (Table 2; for full results and code, see GitHub files and Supplementary Data S4).

Average Akaike weight of the two-rate BM model was >95% for body mass, wing length:body mass ratio, tarsus length:body mass ratio, rachis width:length, barb density (trailing:leading), and leading barb length, but only 61% for trailing:leading barb angle ratio and 59% for trailing:leading barb length ratio.

For all traits except barb length ratio, flightless taxa had higher average rate of phenotypic change. Body mass showed an average flightless rate of 0.57 and volant rate of 0.02, with 91/100 character histories favoring faster flightless rates. Wing length:body mass ratios showed an average flightless rate of 1.71 and volant rate of 0.01, with 96 character histories showing higher rates in flightless taxa. Tarsus length:body mass showed an average flightless rate of 0.41 and volant rate of 0.02, with 89/100 character histories favoring faster flightless rates. Rachis width:length showed an average rate of 0.19 for flightless species and <0.01 for volant species, with all stochastically mapped character histories favoring faster rates in flightless species.

Mixture model regression

Barb density shows an overall relationship between trailing and leading density measures, but no clear effects resulting from flightlessness in these regressions (Figure 5; Table 3). Trailing and leading barb length tightly correlate, with credible differences in both intercept and slope with flight loss (Figure 5; Table 3). There is no clear relationship between trailing and leading barb angles in flying birds (Figure 5; Table 3), while there is a credible ~1:1 relationship between these angles in flightless birds. Wing length relative to mass shows no clear differences in slope or intercept with flight loss, but there was credible difference in evolutionary rate of the wing:mass relationship (higher in flightless taxa; Figure 5; Table 3). Here, evolutionary rates describe how quickly lineages diverge along the regression line estimated by two traits (e.g., mass and wing length), rather than within one-dimensional trait-space of single-trait estimates in Table 2 (for full results and code, see GitHub files and Supplementary Data S4).

Sampling error

To evaluate potential effects of measurement error and within-species variation, we undertook several analyses beyond incorporating the maximum inter-individual standard error for each trait in our phylogenetic rate estimates (Supplementary Data S5). First, we compared 14 microscopic measurements of the same nine specimens recorded by two different observers to judge measurement error. Median percent change from one observer to the other ranged only from ~12.6% for barbule length to ~0.06% for rachis length. Measurement precision between the two observers improved at larger scale.

Second, intra-individual variation in feather asymmetry was examined using data from Feo et al. (2015). Asymmetry was calculated as percent change from the leading to the trailing vane for three metrics: vane width, barb length, and barb angle. Their extant dataset contains 60 volant species, with each species represented by a single individual. For each volant individual, we combined their data recorded from the

Table 2. Evolutionary rates estimated from a 2-rate Brownian Motion model and support for the 2-rate model over the 1-rate model estimated for the standardized values of each trait using OUwie.

	Mass	Wing:Mass	Tarsus:Mass	Rachis Width:Length	Barb density Trail:Lead	Barb length Trail:Lead	Barb angle Trail:Lead	Barb length (lead)
Average intraspecific variation	0.01	0.01	0.01	0.17	0.09	0.13	0.17	0.27
Volant rate (sigma^2)	0.02	0.01	0.02	0	0.02	0.02	0.02	0.01
Flightless rate (sigma^2)	0.57	1.71	0.41	0.19	1.88	0.08	0.08	0.19
Number of SIMMAPs favoring 2-rate	91	96	89	100	97	74	98	100
Mean Akaike weight of 2-rate model	0.99	1	0.966	1	0.985	0.591	0.607	0.993

Note. Rates are in interspecific standard deviation units and directly comparable between traits. Average intraspecific variation values for mass, wing:mass, and tarsus:mass from Weeks et al. (2020). Intraspecific variation values for microscopic traits from our repeated measurements of flying and flightless *Fulica* species.

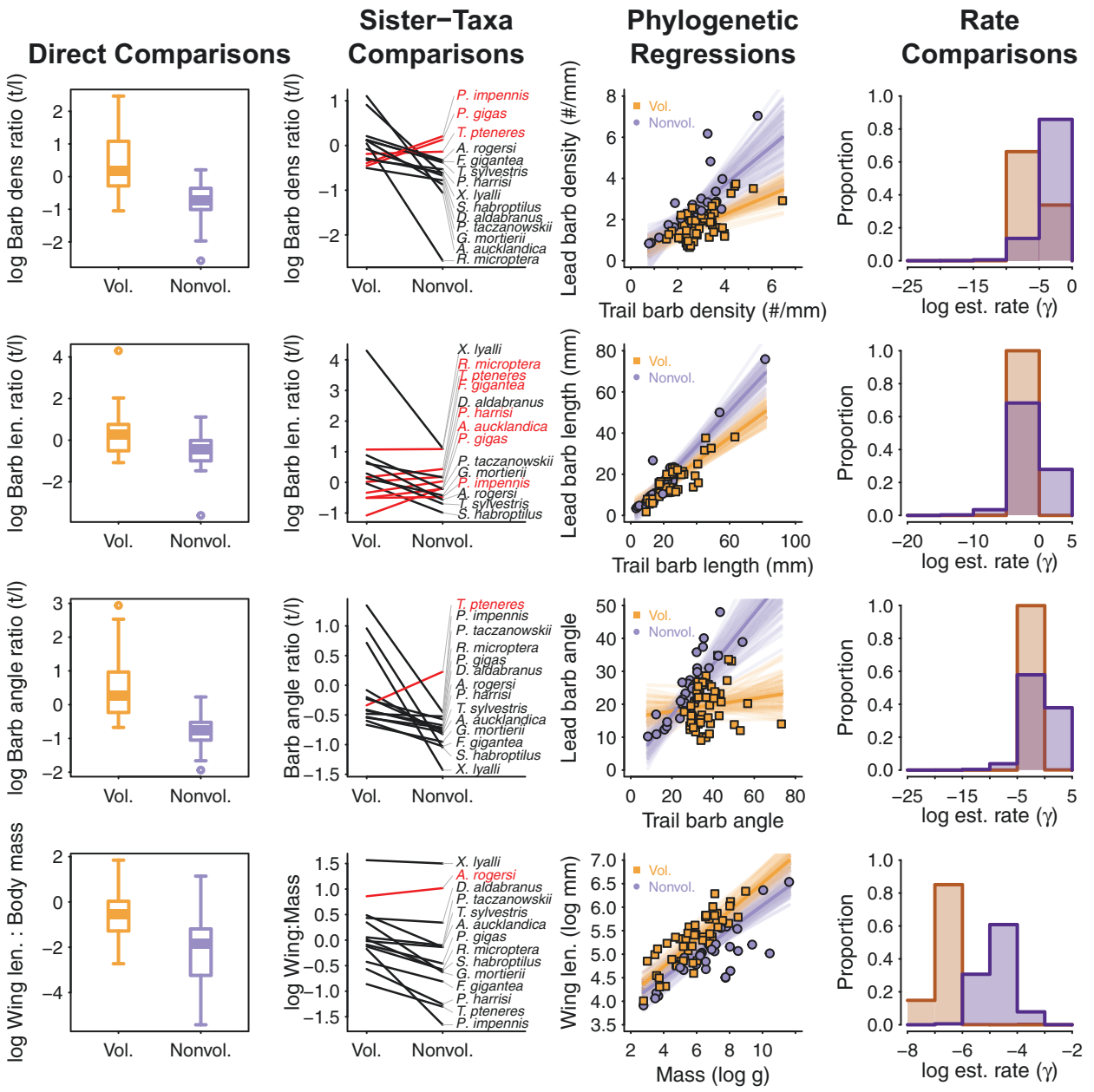

Figure 5. Phylogenetic comparative methods results summary. Each row displays a series of increasingly complex analyses, from simple comparison of standardized trait values between volant and flightless taxa (left) and between sister taxa (left center) to results from mixture model regression for raw trait values showing 100 posterior draws of regressions coefficients (right center) and full posterior distributions for phenotypic rates (right). Top row shows barb densities, second row shows barb lengths, third row shows barb angles, and fourth row shows wing length relative to mass. Orange represents volant species, purple represents flightless species. In sister taxa comparisons, red lines indicate increase in the trait with flight loss, while black lines indicate decrease in that trait. Poor-flying/"incipientlyflightless" *Mergus australis* coded here as volant. Unknown flyer *Mesitornis unicolor* coded here as flightless. $N = 82$ taxa for all but immediate sister taxa comparisons, which are 14 pairs of volant and flightless comparisons.

three primaries at the two points along each primary, yielding a total of six values of percent change per individual for each asymmetry metric (i.e., asymmetry calculated at two positions each on three feathers). Within each individual, we calculated standard deviations of percent change for the three asymmetry metrics. For each flightless individual, Feo et al. (2015) only measured one primary at one point along the primary, so no standard deviations could be calculated. Intra-individual standard deviation of percent change in vane width from leading to trailing vane had a median value of ~187 percentage points across all 60 volant species. However, intra-individual variation in the other measures of feather asymmetry is less variable. Median intra-individual standard deviation of percent change in barb length and barb angle from leading to trailing vane are, respectively, only ~37 and ~65 percentage points across the 60 volant species. Barb length and barb angle are both metrics used herein, while vane width was not measured, presumably lowering the uncertainty in our results.

Third, we measured four additional volant *Fulica armillata* and four additional flightless *Fulica gigantea*, the sister taxa pair with the largest available sample size. We examined intraspecific variation in 10 key macroscopic and microscopic variables between these five specimens of each species, focusing on traits related to feather symmetry. Both unscaled and

Table 3. Regression coefficients of mixture model fit following Fuentes-G et al. (2020).

	Barb density	Barb length	Barb angle	Wing size
Intercept (volant; β0)	0.34 (–0.37, 1.1)	2.8 (–1, 6.7)	**16 (8.1, 24)**	**3.5 (3.2, 3.9)**
Slope (volant; β1)	**0.48 (0.25, 0.71)**	**0.58 (0.47, 0.69)**	9.6e-02 (–1e-01, 0.29)	**3e-01 (0.25, 0.35)**
Group effect (β2)	–0.41 (–1.7, 0.87)	**–3.3 (–6.5, –8.7e-02)**	**–15 (–25, -4.1)**	–6.4e-02 (–0.47, 0.37)
Interaction effect (β3)	0.46 (–3.6e-03, 0.92)	**0.27 (0.11, 0.44)**	**0.67 (0.34, 1)**	–4.1e-02 (–0.11, 2.6e-02)
Volant rate (γ1)	6.4e-03 (4.2e-03, 8.9e-03)	0.28 (0.16, 0.42)	5e-01 (0.32, 0.71)	1.2e-03 (7.1e-04, 1.7e-03)
Flightless rate (γ2)	2.4e-02 (1.8e-11, 6.4e-02)	0.79 (2.8e-08, 1.9)	1.1 (8.8e-10, 3.5)	1e-02 (2.3e-03, 2.1e-02)
Phylogenetic signal (λ)	0.14 (0, 5e-01)	0.81 (0.56, 0.97)	0.27 (0, 0.69)	0.84 (0.66, 1)
log(γ1) – log(γ2)	–0.91 (–3, 1.5)	–5e-01 (–2.7, 3.5)	0.18 (–2.7, 4.2)	**–2 (–3.1, –0.93)**

Note. Posterior means and high posterior density intervals (HDIs) for each parameter and trait are shown. β parameters with HDIs excluding zero are bolded. As phenotypic rates cannot include zero, HDI for the log difference in volant and flightless rates is given in final row. Given the particular taxon sampling of this tree, phylogenetic signal parameter λ cannot be interpreted as it would in a tree with comprehensive or random taxon sampling.

scaled wing length show a difference in means between the two species greater than the sum of their standard deviations. For each of three microscopic measures related to feather asymmetry, differences between the species means exceed the summed standard deviations of the two species.

Discussion

Flightless taxa have more diverse feather morphologies; flight feathers are more robust than contours

PCA of linear feather metrics across the plumage shows greater overall diversity of feather morphologies in flightless taxa, suggesting release of selective pressure from flight requirements and exaptation of feathers previously used in flight to alternative primary functions (e.g., swimming). The pattern from primary, rectrix, tertial, dorsal contour, to ventral contour in terms of shorter/wider filaments to relatively longer/thinner filaments indicates that our measurements indeed capture functional signals. More robust feathers (i.e., short filaments relative to rachis width) play a greater role in locomotion (flight or swimming) and less robust feathers play a greater role in thermoregulation and other functions (Terrill & Shultz, 2023). Furthermore, the least robust remiges and rectrices are more often from terrestrial taxa rather than semiaquatic taxa, which sometimes use their feathers for locomotion in the dense medium of water even when flightless. These least robust remiges and rectrices appear at the bottom-right edge of the morphospace (Figure 2D), with the lowest PC2 values and high PC1 values; they are not the contours with the lowest PC1 values.

Extreme feather modification in ancient flightless lineages

Ratites show diverse shifts in primary feather morphology. Some shift towards long filaments, while others reduce their filaments, sometimes losing filaments entirely (e.g., cassowary primaries lack barbules and barbs). The diversity of ratite feather morphologies is consistent with release from selective pressure. Their forelimbs and pectoral gridles are often greatly reduced and minimally used (Cubo & Arthur, 2001; Habib & Ruff, 2008; Lowi-Merri et al., 2021; Novas et al., 2020; Nudds et al., 2004; Serrano et al., 2020), while enough evolutionary time has passed to allow for developmental constraints on feather development to be overcome. Filament loss (i.e., loss of fractal branching) may indicate that feathers are functioning more analogously to morphologically simpler mammalian hair, providing thermoregulation, camouflage, abrasion resistance, and/or water repellency rather than locomotion (although *Struthio* feathers are an exception and function in display [Bolwig, 1973]).

Wide filaments, and especially wide rachises, in penguins possibly result from a shift in selection (Lahti et al., 2009) for locomoting in the dense medium of water and a shift towards small, scale-like feathers as the wings adapt into a hydrodynamic flipper.

Barb angles reveal increased flight feather symmetry upon flight loss

Feather symmetry differences between sister taxa agree with previous reports that primary vane asymmetry is an adaptation for flight (Feduccia & Tordoff, 1979; Feo et al., 2015). Primaries, but not other feather positions, of flightless taxa are markedly more symmetric than in their closest volant relatives. It is unsurprising that the most prominent increases in feather symmetry occur in ratites and penguins; they are highly specialized terrestrial taxa and underwater "flyers" with long evolutionary histories of flightlessness. Ratites long ago lost forelimb locomotor function, while underwater "flying" penguins ultimately transformed their wings into flippers (i.e., a proportionally fleshier "waterfoil," rather than a more keratinous airfoil).

Unscaled filament densities decrease upon flight loss, but scaling confounds; signal of increased feather symmetry persists

In sister taxon comparisons, the tendency to decrease (unscaled) filament densities upon losing flight is consistent with releasing selection pressure for maintaining tightly packed, well-zipped airfoils. Relatedly, trailing barbule spacing is constant across diverse volant species, despite their mass (Sullivan et al., 2017). All feather positions show density decreases. In terrestrial flightless taxa, this might reflect released selection pressure for aerodynamic plumage across the body, including contour feathers. In semiaquatic flightless taxa, the density and cohesion of water might not require tight barb/barbule packing to function as a hydrofoil, or wider/stiffer barbs might be selected for in this dense medium.

The above interpretations might be influenced by overall feather size. Ratites other than kiwis can have very large feathers, while penguins have very small feathers. Overall

body mass typically increases with flightlessness, possibly leading to increased feather size and associated filament density decline in large ratites. Although penguins are massive, they have small, scale-like feathers expected to show increased filament densities under isometric scaling. Penguin feathers are hydrophobically water- and ice-shedding due to tight interweaving of filaments, down to hooklets/barbicels of barbules (Wood et al., 2022) consistent with their increased unscaled filament densities.

When densities are scaled to rachis width, results are similar. Filament densities further support the impact of flight loss on feather symmetry. Increased barb densities in leading vanes of primaries is unsurprising since feather asymmetry decreases upon flight loss. Higher branching angles allow for easier barb packing along the rachis. Increased feather symmetry after flight loss reflected in leading and trailing barb densities appears in PCM, suggesting these results persist even when accounting for body mass.

Tight phylogenetic control shows body mass, wing length, and feather symmetry are impacted by flight loss

PCM support the partially corrected analyses and identify the most prominent evolutionary changes upon flight loss. Macroscopically, body mass increase and wing length (relative to body mass) decrease are most strongly associated with flight loss. Microscopically, increased feather symmetry observed in ratios of leading/trailing barb lengths, angles, and densities is most strongly associated with flight loss. Correlation between flight loss and these macro- and microscopic traits appears repeatedly across our series of analyses. The pattern is complicated by the side of the vane analyzed, as the relationship between trailing and leading barb density and angle changes upon flight loss. In flying birds, leading and trailing barb angles are unrelated to one another, implying they evolve to optimize feather shape. In flightless taxa, the two are tightly correlated—potentially suggesting developmental constraint.

Rates of evolution for traits most strongly correlated with flightlessness (Figure 5A) indicate that flight loss induces novel evolution in these traits, likely due to relaxed selection pressures relating to flight and shifts toward primary functions other than flight (e.g., swimming, thermoregulation).

Relaxed selection on complex traits: feather developmental stages and flight loss

Evolutionary changes in feathers after flight loss might relate to underlying developmental processes. In common models of feather development (Prum, 2005; Prum & Brush, 2002), changes in feather morphology after flight loss likely occur in reverse order of this "evo-devo" model. Stage Va (asymmetric flight feathers) is the most readily lost or altered stage after flight loss, reverting toward symmetric Stage IV. This implies loss of lateral displacement of new barb loci in the feather follicle. After many millions of years of flightless, vanes can change from closed to open (reverting from Stage IV to IIIa+b with loss of differentiated distal and proximal barbules) and barbules can be lost (reverting from Stage IIIa+b to IIIa with loss of periphal barbule plates), as in the feathers of various ratites. Cassowary primary feathers lost barbs to produce a quill-like, bare rachis, showing further reversion from Stage IIIA all the way to Stage I, with complete loss of barb ridges. Later stages of feather development (e.g., lateral displacement of barb loci in the follicle) are more liable to developmental truncation or modification than are early stages (e.g., barb ridge differentiation in the follicle collar), consistent with apical modification/loss. The very different timescales for proximate and distant trait changes after flight loss indicate that feather evolution is highly conserved and developmentally constrained.

Relaxed selection occurs in various contexts such that partial or total loss of trait function ultimately leads to lost, vestigial, or relict traits (Lahti et al., 2009) (e.g., lost eyes and pigments in cavefish [Jeffery, 2005]). Flight loss commonly occurs in two ecological contexts (island or semiaquatic), but the complex structure/development of feathers yields interesting patterns of trait retention versus modification over time, and modification rate might correlate to developmental sequence.

Patterns of trait evolution under relaxed selection, as related to fitness, are expected to vary according to several models (Figure I in Lahti et al., 2009). Our results show that the most immediate effect of relaxed selection on feathers after flight loss is reversion to symmetry. Without selection on barb angles for different functions, they revert to more basic, linked development. This pattern matches the "neutral" model of Lahti et al. (2009; Figure IB therein), where increased feather complexity is not favored or at least developmentally constrained, while decreased complexity is neutral and permitted (Haldane, 1933). An example of this relaxed selection model would be predator escape behavior in predator-free environments (Lahti et al., 2009)—relevant to many island-founding flightless birds.

Beyond becoming symmetrical, feathers exhibit slow rates of change (i.e., persistence [Lahti et al., 2009]). On very long timescales, reduction/simplification occurs (e.g., reduced branching in kiwi or ostrich), with total loss of branching in cassowary primaries possibly representing a vestigial structure. Disparate feather morphologies of ratites indicate that relaxed selection in terrestrial flightless taxa widens feather morphology fitness peaks (Lahti et al., 2009).

Feathers are never lost, however, and most modifications are seen in divergences that are tens-of-millions-of-years old. According to Lahti et al. (2009), persistence/evolutionary lag of nonfunctional traits may be explained by either (1) low genetic variation, (2) low cost, or (3) low gene flow from populations with functional traits, with low cost of feathers as the best explanation for feather evolution following flight loss. Lahti et al. (2009) state, "In cases where a reduction in the trait value is selectively neutral…, neutral evolutionary mechanisms will predominate, and trait decay should be gradual and slow" (p. 493). Unlike cavefish losing eyes over 10,000 years while enhancing other senses (Jeffery, 2005), there seems to be no obvious trade-off for simplifying/reducing low-cost remiges, so complex development is maintained for millions of years.

Relaxing selection from one source can allow others to gain relative importance (Lahti et al., 2009), as is likely the case for semiaquatic flightless birds that change wing function from aerial to underwater "flight." In auks, razorbills have both aerial and underwater "flight," and sister taxon comparisons suggest aerial flight selection constrains feathers to resemble those of other volant taxa. When Great Auks lost flight, their flight feathers were dramatically reduced. Modeling suggests that relaxed selection enables adaptive pathways requiring multiple deleterious steps to cross fitness valleys (Draghi et

al., 2024), possibly explaining why highly modified penguin feathers evolved novel, specialized functions after extended periods of relaxed selection for aerial flight.

Paleobiological implications

Did some fully terrestrial nonavian dinosaurs have aerially locomoting ancestors (Kiat & O'Connor, 2024; Longrich, 1998; Paul, 2002), such that similar evolutionary tendencies toward repeated flight loss seen in crown group birds yielded multiple independent losses of gliding/flight in stem avians? Changes in size and skeletomusculature (e.g., relative wing length) occur more rapidly than most changes in feather anatomy, consistent with some patterns in the fossil record. For example, small microraptorines (e.g., *Microraptor*) were likely capable of aerial locomotion (Pei et al., 2020), but microraptorines over ~50 kg (e.g., *Tianyuraptor*, *Zhanyuanlong*) were short-armed and possibly incapable of aerial locomotion, despite retaining long (>35 cm), asymmetric primaries (Lü & Brusatte, 2015) consistent with a gliding/flying ancestor.

Although reversals to more symmetric vanes in remiges occur after flight loss in crown group birds, their evolutionary rate is lower than those for increased mass or decreased relative wing length. Kiat and O'Connor's (2024) suggestion that mid-Jurassic anchiornithines were secondarily "flightless" and exhibited a reversal in remex vane symmetry should therefore be reconsidered. Under their interpretation, the first appearance of asymmetric primaries would be pushed back to the Early Jurassic, where fossil evidence for Paraves (i.e., most inclusive clade containing birds and anchiornithines) is currently lacking and only disputed evidence (Xu et al., 2001) for broader clades (e.g., Maniraptora) exists. Our results and "evo-devo" models of feathers (Prum, 2005) suggest that anchiornithine remex symmetry represents the ancestral condition. Still, wing architecture (e.g., size, structure, and distribution of feather types) in anchiornithines differs from those of crown birds (Kiat & O'Connor, 2024; Longrich et al., 2012; Saitta et al., 2018). Wings of achiornithines and other nonavian theropods likely functioned differently as airfoils compared to crown birds.

Conclusion

Among birds, flight loss strongly correlates with increased body mass and decreased wing length relative to body mass. Without selection for flight, the upper limit on body mass rises, compounded by supportive buoyancy of water on semiaquatic flightless taxa. Unlike these macroscopic traits, many feather microstructural traits (except feather asymmetry) are less likely to change, at least soon after flight loss. As continually shed and regenerated extracellular integumentary corneous beta-protein ("keratin") (Holthaus et al., 2018), feathers are likely not as metabolically costly as flight skeletomusculature and may be under comparatively relaxed selection in flightless taxa. In conjunction with this selection hypothesis, constraints imposed by complex hierarchical developmental processes may prevent feathers from rapidly evolving. Regarding locomotory selective pressures, semiaquatic flightless taxa experience both selection for swimming and relaxed selection for flight.

The most prominent microscopic changes after flight loss occur in flight feathers, especially primaries. Feather asymmetry decreases even in species that have been flightless for less than a million years. We might hypothesize that, early in the evolution of flightless taxa, primary remex filaments typically lengthen (Supplementary Material, Section 7) and, in semiaquatic flightless taxa, rachis width increases (perhaps maintaining feather shape in water). These patterns, if present, are less prominent than decreased feather asymmetry.

A neutral model of relaxed selection and low cost of complex feather production (i.e., lacking major tradeoffs) means that persistence of complex feather morphology lasts over millions of years, constrained by developmental processes in the follicle. Late in the evolution of flightless lineages (i.e., taxa that diverged from volant ancestors tens-of-millions of years ago), the most prominent shift to symmetric feathers occurs. Ratites show diverse feather morphotypes. Some have large feathers (except kiwis), shaggy plumage, and low unscaled filament density. Ostrich have plumulaceous primary remiges. Cassowary feathers lost many barbules. In cassowary primaries, even barbs are lost, producing what might be considered a vestigial flight feather. Except ostrich primaries, for example, ratite feathers tend toward filament reduction. Shaggy plumage and feather simplification in ratites suggest that terrestrial flightless bird feathers function more akin to nonbranching mammalian hair, given sufficient evolutionary time to overcome developmental constraints. Relaxing selection for aerial flight allows for other functions to become prominent. In some semiaquatic taxa, "flight" is shifted underwater to produce novel feather morphologies with unique functions, rather than the diversity seen in ratite feathers. Penguins evolve robust, scale-like feathers with wide filaments, small overall size, and high unscaled filament density. Their hydrofoil for lift and thrust during swimming is relatively fleshier than feathered, and their feathers have ice-shedding capability.

Some signatures of secondary flightlessness repeatedly appear across independent lineages, but there may be differences based on ecological context (i.e., terrestrial versus semiaquatic). Skeletal, rather than feather, anatomy (perhaps excepting feather symmetry) is the better indicator of flight loss in extinct taxa, especially if flight loss was evolutionarily recent—consistent with relationships between coracoid strength and wing-beat propulsion in birds (Akeda & Fujiwara, 2022). Somewhat predictable changes in feathers still occur, especially given sufficient evolutionary time. Feather evolution after flight loss generally occurs in reverse order of commonly invoked developmental models for feathers, suggesting strong developmental constraints.

Supplementary material

Supplementary material is available online at *Evolution*.

Data availability

Raw data, supplementary results, and code are available as supplementary material files and have also been archived on Dryad at DOI: 10.5061/dryad.qrfj6q5s7. Data and code for the phylogenetic comparative analyses are also available on GitHub at https://github.com/paleomitchelljs/FeatherEvo

Author contributions

E.T.S. and P.J.M. conceived the project. E.T.S. and L.B. collected data. E.T.S. and J.S.M. performed statistical analyses. All authors contributed to writing the manuscript.

Funding

Research was supported by the Bass postdoctoral research fund at the Field Museum. We thank the Jeff Metcalf Internship Program (University of Chicago) for supporting L.B. P.J.M.'s research was supported by the National Science Foundation EAR 1925884.

Conflict of interest: The authors declare no conflict of interest.

Acknowledgments

We thank the following at the FMNH for access to the bird collections and helpful discussion: Ben Marks, John Bates, and Shannon Hackett. Furthermore, we thank the following at the AMNH for access to their bird collections and helpful discussion: Bentley Bird and Paul Sweet. We also thank Andrew Romanelli for assistance in data collection. We thank two anonymous referees and the journal editorial staff for their helpful feedback.

Silhouettes in main text and supplement are from phylopic.org: *Pinguinus impennis* modified from John James Audubon (Public Domain Mark 1.0), *Xenicus* by Wynston Cooper (photo) and Albert Chen (a.k.a. "Albertonykus") (silhouette) (CC BY-SA 3.0), *Aptenodytes* by Steven Traver (Public Domain Mark 1.0), *Phalacrocorax* by L. Shyamal (CC BY-SA 3.0), *Podiceps* by Doug Backlund (photo), John E. McCormack, Michael G. Harvey, Brant C. Faircloth, Nicholas G. Crawford, Travis C. Glenn, Robb T. Brumfield & T. Michael Keesey (CC BY-SA 3.0), Anatidae by Rebecca Groom (CC BY-SA 3.0), *Apteryx australis* by Steven Traver (Public Domain Mark 1.0), *Casuarius* by Ferran Sayol (Public Domain Mark 1.0), *Dromaius novaehollandiae* by Darren Naish (vectorized by T. Michael Keesey) (CC BY-SA 3.0), *Struthio camelus* by Ferran Sayol (Public Domain Mark 1.0), Rhea americana by Ferran Sayol (Public Domain Mark 1.0), *Nestor notabilis* by Ferran Sayol (Public Domain Mark 1.0), Gallirallus australis by T. Michael Keesey (vectorization) and HuttyMcphoo (photography) (CC BY-SA 3.0).

References

Akeda, T., & Fujiwara, S. I. (2022). Coracoid strength as an indicator of wing-beat propulsion in birds. *Journal of Anatomy*, *242*(3), 436–446. https://doi.org/10.1111/joa.13788

Amrhein, V., Greenland, S., & McShane, B. (2019). Scientists rise up against statistical significance. *Nature*, *567*(7748), 305–307. https://doi.org/10.1038/d41586-019-00857-9

Barrowclough, G. F., Cracraft, J., Klicka, J., & Zink, R. M. (2016). How many kinds of birds are there and why does it matter? *PLoS One*, *11*(11), e0166307. https://doi.org/10.1371/journal.pone.0166307

Beaulieu, J. M., Jhwueng, D. C., Boettiger, C., & O'Meara, B. C. (2012). Modeling stabilizing selection: Expanding the Ornstein–Uhlenbeck model of adaptive evolution. *Evolution*, *66*(8), 2369–2383. https://doi.org/10.1111/j.1558-5646.2012.01619.x

Beaulieu, J. M., O'Meara, B., & Beaulieu, M. J. (2016). *Package 'OUwie'*. R Packag. version, 1, pp. 1–19.

Bolwig, N. (1973). Agonistic and sexual behavior of the African Ostrich (*Struthio camelus*). *The Condor*, *75*(1), 100–105. https://doi.org/10.2307/1366538

Bürkner, P. (2018). Advanced Bayesian multilevel modeling with the R package brms. *The R Journal*, *10*(1), 395–411. https://doi.org/10.32614/rj-2018-017

Bürkner, P. (2021). Bayesian item response modeling in r with brms and Stan. *Journal of Statistical Software*, *100*(5), 1–54.

Bürkner, P. C. (2017). brms: An R package for Bayesian multilevel models using Stan. *Journal of statistical software*, *80*(1), 1–28.

Chernova, O. F., & Kiladze, A. B. (2019). Heterochrony as the basis for inter-and intraspecific diversity of skin in vertebrates. *Biology Bulletin Reviews*, *9*(2), 174–189. https://doi.org/10.1134/s207908641902004x

Clout, M. N., & Craig, J. L. (1995). The conservation of critically endangered flightless birds in New Zealand. *Ibis*, *137*(s1), S181–S190.

Cubo, J., & Arthur, W. (2001). Patterns of correlated character evolution in flightless birds: A phylogenetic approach. *Evolutionary Ecology*, *14*(8), 693–702. https://doi.org/10.1023/a:1011695406277

de Villemereuil, P. D., Wells, J. A., Edwards, R. D., & Blomberg, S. P. (2012). Bayesian models for comparative analysis integrating phylogenetic uncertainty. *BMC Evolutionary Biology*, *12*, 1–16.

Dial, K. P., & Heers, A. M. (2021). Waxing and waning of wings. *Trends in Ecology & Evolution*, *36*(5), 457–470. https://doi.org/10.1016/j.tree.2021.01.006

Draghi, J. A., Ogbunugafor, C. B., Zaman, L., & Parsons, T. (2024). Relaxed selection can speed the evolution of complex adaptations. *bioRxiv* 602773. https://doi.org/10.1101/2024.07.09.602773, July 09, 2024, preprint: not peer reviewed.

Dunning, J. J. B. (2008). *CRC handbook of avian body masses* (2nd ed.). CRC Press.

Elliott, K. H., Ricklefs, R. E., Gaston, A. J., Hatch, S. A., Speakman, J. R., & Davoren, G. K. (2013). High flight costs, but low dive costs, in auks support the biomechanical hypothesis for flightlessness in penguins. *Proceedings of the National Academy of Sciences of the United States of America*, *110*(23), 9380–9384. https://doi.org/10.1073/pnas.1304838110

Feduccia, A., & Tordoff, H. B. (1979). Feathers of *Archaeopteryx*: Asymmetric vanes indicate aerodynamic function. *Science*, *203*(4384), 1021–1022. https://doi.org/10.1126/science.203.4384.1021

Feng, C., Gao, Y., Dorshorst, B., Song, C., Gu, X., Li, Q., Li, J., Liu, T., Rubin, C. J., Zhao, Y., Wang, Y., Fei, J., Li, H., Chen, K., Qu, H., Shu, D., Ashwell, C., Da, Y., Andersson, L., … Li, N. (2014). A cis-regulatory mutation of PDSS2 causes silky-feather in chickens. *PLoS Genetics*, *10*(8), e1004576. https://doi.org/10.1371/journal.pgen.1004576

Feo, T. J., Field, D. J., & Prum, R. O. (2015). Barb geometry of asymmetrical feathers reveals a transitional morphology in the evolution of avian flight. *Proceedings Biological Sciences*, *282*(1803), 20142864. https://doi.org/10.1098/rspb.2014.2864

Feo, T. J., & Prum, R. O. (2014). Theoretical morphology and development of flight feather vane asymmetry with experimental tests in parrots. *Journal of Experimental Zoology. Part B. Molecular and Developmental Evolution*, *322*(4), 240–255. https://doi.org/10.1002/jez.b.22573

Feo, T. J., Simon, E., & Prum, R. O. (2016). Theory of the development of curved barbs and their effects on feather morphology. *Journal of Morphology*, *277*(8), 995–1013. https://doi.org/10.1002/jmor.20552

Fish, F. E. (2016). Secondary evolution of aquatic propulsion in higher vertebrates: Validation and prospect. *Integrative and Comparative Biology*, *56*(6), 1285–1297. https://doi.org/10.1093/icb/icw123

Fjeldså, J. (1981). Biological notes on the giant coot *Fulica gigantea*. *Ibis*, *123*(4), 423–437. https://doi.org/10.1111/j.1474-919x.1981.tb04047.x

Fuentes-G, J. A., Polly, P. D., & Martins, E. P. (2020). A Bayesian extension of phylogenetic generalized least squares: Incorporating uncertainty in the comparative study of trait relationships and evolutionary rates. *Evolution*, *74*(2), 311–325. https://doi.org/10.1111/evo.13899

Fulton, T. L., Letts, B., & Shapiro, B. (2012). Multiple losses of flight and recent speciation in steamer ducks. *Proceedings Biological Sciences*, *279*(1737), 2339–2346. https://doi.org/10.1098/rspb.2011.2599

Garcia-Ramirez, J. C., & Matzke, N. J. (2021). Trait-dependent dispersal in rails (Aves: Rallidae): Historical biogeography of a cosmopolitan bird clade. *Molecular Phylogenetics and Evolution*, *159*, 107106.

Habib, M. B., & Ruff, C. B. (2008). The effects of locomotion on the structural characteristics of avian limb bones. *Zoological Journal of the Linnean Society*, *153*(3), 601–624. https://doi.org/10.1111/j.1096-3642.2008.00402.x

Haldane, J. B. S. (1933). The part played by recurrent mutation in evolution. *The American Naturalist*, *67*(708), 5–19. https://doi.org/10.1086/280465

Holthaus, K. B., Eckhart, L., Dalla Valle, L., & Alibardi, L. (2018). Evolution and diversification of corneous beta-proteins, the characteristic epidermal proteins of reptiles and birds. *Journal of Experimental Zoology. Part B. Molecular and Developmental Evolution*, *330*(8), 438–453. https://doi.org/10.1002/jez.b.22840

Humphrey, P. S., & Livezey, B. C. (1982). Flightlessness in flying steamer-ducks. *The Auk*, *99*(2), 368–372.

IUCN. 2022. *The IUCN Red List of Threatened Species*. Version 2022-2. https://www.iucnredlist.org

Jeffery, W. R. (2005). Adaptive evolution of eye degeneration in the Mexican blind cavefish. *The Journal of Heredity*, *96*(3), 185–196. https://doi.org/10.1093/jhered/esi028

Jetz, W., Thomas, G. H., Joy, J. B., Hartmann, K., & Mooers, A. O. (2012). The global diversity of birds in space and time. *Nature*, *491*(7424), 444–448. https://doi.org/10.1038/nature11631

Kelley, N. P., & Pyenson, N. D. (2015). Evolutionary innovation and ecology in marine tetrapods from the Triassic to the Anthropocene. *Science*, *348*(6232), aaa3716. https://doi.org/10.1126/science.aaa3716

Kiat, Y., & O'Connor, J. K. (2024). Functional constraints on the number and shape of flight feathers. *Proceedings of the National Academy of Sciences of the United States of America*, *121*(8), e2306639121. https://doi.org/10.1073/pnas.2306639121

Kruschke, J. K. (2011). *Doing Bayesian data analysis. A tutorial with R and BUGS*. Academic Press/Elsevier.

Ksepka, D. T., Balanoff, A. M., Smith, N. A., Bever, G. S., Bhullar, B. A. S., Bourdon, E., Braun, E. L., Burleigh, J. G., Clarke, J. A., Colbert, M. W., & Corfield, J. R. (2020). Tempo and pattern of avian brain size evolution. *Current Biology*, *30*(11), 2026–2036.

Ksepka, D. T., Bertelli, S., & Giannini, N. P. (2006). The phylogeny of the living and fossil Sphenisciformes (penguins). *Cladistics*, *22*(5), 412–441. https://doi.org/10.1111/j.1096-0031.2006.00116.x

Lahti, D. C., Johnson, N. A., Ajie, B. C., Otto, S. P., Hendry, A. P., Blumstein, D. T., Coss, R. G., Donohue, K., & Foster, S. A. (2009). Relaxed selection in the wild. *Trends in Ecology & Evolution*, *24*(9), 487–496. https://doi.org/10.1016/j.tree.2009.03.010

Lin, C. M., Jiang, T. X., Widelitz, R. B., & Chuong, C. M. (2006). Molecular signaling in feather morphogenesis. *Current Opinion in Cell Biology*, *18*(6), 730–741. https://doi.org/10.1016/j.ceb.2006.10.009

Livezey, B. C. (1989). Phylogenetic relationships and incipient flightlessness of the extinct Auckland Islands Merganser. *The Wilson Bulletin*, *101*(3), 410–435.

Livezey, B.C. (2003). *Evolution of flightlessness in rails (Gruiformes, Rallidae)*. American Ornithologists' Union.

Lomolino, M. V., van der Geer, A. A., Lyras, G. A., Palombo, M. R., Sax, D. F., & Rozzi, R. (2013). Of mice and mammoths: Generality and antiquity of the island rule. *Journal of Biogeography*, *40*(8), 1427–1439. https://doi.org/10.1111/jbi.12096

Longrich, N. R. (1998). *Secondary Flightlessnes in Basal Maniraptoran Theropods*. Princeton University Senior Thesis.

Longrich, N. R., Vinther, J., Meng, Q., Li, Q., & Russell, A. P. (2012). Primitive wing feather arrangement in *Archaeopteryx lithographica* and *Anchiornis huxleyi*. *Current Biology: CB*, *22*(23), 2262–2267. https://doi.org/10.1016/j.cub.2012.09.052

Lowi-Merri, T. M., Benson, R. B., Claramunt, S., & Evans, D. C. (2021). The relationship between sternum variation and mode of locomotion in birds. *BMC Biology*, *19*(1), 1–23.

Lü, J., & Brusatte, S. L. (2015). A large, short-armed, winged dromaeosaurid (Dinosauria: Theropoda) from the Early Cretaceous of China and its implications for feather evolution. *Scientific Reports*, *5*, 11775. https://doi.org/10.1038/srep11775

Maderson, P. F., & Alibardi, L. (2000). The development of the sauropsid integument: A contribution to the problem of the origin and evolution of feathers. *American Zoologist*, *40*(4), 513–529.

McGowan, C. (1989). Feather structure in flightless birds and its bearing on the question of the origin of feathers. *Journal of Zoology*, *218*(4), 537–547. https://doi.org/10.1111/j.1469-7998.1989.tb04997.x

Meredith, M., & Kruschke, J. (2022). *HDInterval: Highest (Posterior) Density Intervals*. R package version 0.2.4, https://CRAN.R-project.org/package=HDInterval

Miller, W. J. (1956). Silky plumage in the ring neck dove. *Journal of Heredity*, *47*(1), 37–40. https://doi.org/10.1093/oxfordjournals.jhered.a106599

Mitchell, J. S., & Makovicky, P. J. (2014). Low ecological disparity in early cretaceous birds. *Proceedings Biological Sciences*, *281*(1787), 20140608. https://doi.org/10.1098/rspb.2014.0608

Munafò, M. R., & Smith, G. D. (2018). Robust research needs many lines of evidence. *Nature*, *553*, 339–401.

Novas, F. E., Agnolin, F., Brissón Egli, F., & Lo Coco, G. E. (2020). Pectoral girdle morphology in early-diverging paravians and living ratites: Implications for the origin of flight.

Nudds, R. L., Dyke, G. J., & Rayner, J. M. V. (2004). Forelimb proportions and the evolutionary radiation of Neornithes. *Proceedings Biological Sciences*, *271*(Suppl 5), S324–S327. https://doi.org/10.1098/rsbl.2004.0167

Paul, G. S. (2002). *Dinosaurs of the air: The evolution and loss of flight in dinosaurs and birds*. JHU Press.

Pei, R., Pittman, M., Goloboff, P. A., Dececchi, T. A., Habib, M. B., Kaye, T. G., Larsson, H. C., Norell, M. A., Brusatte, S. L., & Xu, X. (2020). Potential for powered flight neared by most close avialan relatives, but few crossed its thresholds. *Current Biology*, *30*(20), 4033–4046.e8. https://doi.org/10.1016/j.cub.2020.06.105

Prum, R. O. (1999). Development and evolutionary origin of feathers. *The Journal of Experimental Zoology*, *285*(4), 291–306.

Prum, R. O. (2005). Evolution of the morphological innovations of feathers. *Journal of Experimental Zoology. Part B. Molecular and Developmental Evolution*, *304*(6), 570–579. https://doi.org/10.1002/jez.b.21073

Prum, R. O., & Brush, A. H. (2002). The evolutionary origin and diversification of feathers. *The Quarterly Review of Biology*, *77*(3), 261–295. https://doi.org/10.1086/341993

Reddy, S., Kimball, R. T., Pandey, A., Hosner, P. A., Braun, M. J., Hackett, S. J., Han, K. L., Harshman, J., Huddleston, C. J., Kingston, S., Marks, B. D., Miglia, K. J., Moore, W. S., Sheldon, F. H., Witt, C. C., Yuri, T., & Braun, E. L. (2017). Why do phylogenomic data sets yield conflicting trees? Data type influences the avian tree of life more than taxon sampling. *Systematic Biology*, *66*(5), 857–879. https://doi.org/10.1093/sysbio/syx041

Revell, L. J. (2012). phytools: An R package for phylogenetic comparative biology (and other things). *Methods in Ecology and Evolution*, *3*(2), 217–223. https://doi.org/10.1111/j.2041-210x.2011.00169.x

Roots, C. (2006). *Flightless birds*. Greenwood Publishing Group.

Saitta, E. T., Gelernter, R., & Vinther, J. (2018). Additional information on the primitive contour and wing feathering of paravian dinosaurs. *Palaeontology*, *61*(2), 273–288. https://doi.org/10.1111/pala.12342

Sawyer, R. H., Washington, L. D., Salvatore, B. A., Glenn, T. C., & Knapp, L. W. (2003). Origin of archosaurian integumentary appendages: The bristles of the wild turkey beard express feather-type β keratins. *Journal of Experimental Zoology. Part B. Molecular and Developmental Evolution*, *297*(1), 27–34. https://doi.org/10.1002/jez.b.17

Serrano, F. J., Costa-Pérez, M., Navalón, G., & Martín-Serra, A. (2020). Morphological disparity of the humerus in modern birds. *Diversity*, *12*(5), 173. https://doi.org/10.3390/d12050173

Sullivan, T. N., Wang, B., Espinosa, H. D., & Meyers, M. A. (2017). Extreme lightweight structures: avian feathers and bones. *Materials Today*, *20*(7), 377–391. https://doi.org/10.1016/j.mattod.2017.02.004

Taylor, S. S., Jamieson, I. G., & Wallis, G. P. (2007). Historic and contemporary levels of genetic variation in two New Zealand passerines with different histories of decline. *Journal of Evolutionary Biology*, *20*(5), 2035–2047. https://doi.org/10.1111/j.1420-9101.2007.01362.x

Terrill, R. S., & Shultz, A. J. (2023). Feather function and the evolution of birds. *Biological Reviews of the Cambridge Philosophical Society*, *98*(2), 540–566. https://doi.org/10.1111/brv.12918

Torres, C. R., & Clarke, J. A. (2018). Nocturnal giants: Evolution of the sensory ecology in elephant birds and other palaeognaths inferred from digital brain reconstructions. *Proceedings Biological Sciences*, *285*(1890), 20181540. https://doi.org/10.1098/rspb.2018.1540

von Meyer, H. (1861). *Archaeopteryx lithographica (*vogel-feder*)* und *Pterodactylus* von Solnhofen. *Neues Jahrbuch für Mineralogie, Geognosie, Geologie und Petrefakten-Kunde, 1861. Neues Jahrbuch für Mineralogie, Geognosie, Geologie und Petrefakten-Kunde*, *1861*, 678–679.

Watanabe, J., Field, D. J., & Matsuoka, H. (2021). Wing musculature reconstruction in extinct flightless auks (*Pinguinus* and *Mancalla*) reveals incomplete convergence with penguins (Spheniscidae) due to differing ancestral states. *Integrative Organismal Biology (Oxford, England)*, *3*(1), obaa040. https://doi.org/10.1093/iob/obaa040

Weeks, B. C., Willard, D. E., Zimova, M., Ellis, A. A., Witynski, M. L., Hennen, M., & Winger, B. M. (2020). Shared morphological consequences of global warming in North American migratory birds. *Ecology Letters*, *23*(2), 316–325. https://doi.org/10.1111/ele.13434

Wood, M. J., Brock, G., Debray, J., Servio, P., & Kietzig, A. M. (2022). Robust anti-icing surfaces based on dual functionality—microstructurally-induced ice shedding with superimposed nanostructurally-enhanced water shedding. *ACS Applied Materials & Interfaces*, *14*(41), 47310–47321. https://doi.org/10.1021/acsami.2c16972

Wright, N. A., Steadman, D. W., & Witt, C. C. (2016). Predictable evolution toward flightlessness in volant island birds. *Proceedings of the National Academy of Sciences of the United States of America*, *113*(17), 4765–4770. https://doi.org/10.1073/pnas.1522931113

Xu, X., Zhao, X., & Clark, J. M. (2001). A new therizinosaur from the Lower Jurassic lower Lufeng Formation of Yunnan, China. *Journal of Vertebrate Paleontology*, *21*(3), 477–483. https://doi.org/10.1671/0272-4634(2001)021[0477:antftl]2.0.co;2

Yonezawa, T., Segawa, T., Mori, H., Campos, P. F., Hongoh, Y., Endo, H., Akiyoshi, A., Kohno, N., Nishida, S., Wu, J., Jin, H., Adachi, J., Kishino, H., Kurokawa, K., Nogi, Y., Tanabe, H., Mukoyama, H., Yoshida, K., Rasoamiaramanana, A., … Hasegawa, M. (2017). Phylogenomics and morphology of extinct paleognaths reveal the origin and evolution of the ratites. *Current Biology: CB*, *27*(1), 68–77. https://doi.org/10.1016/j.cub.2016.10.029